

## ARTICLE

# A frameshift mutation in prominin (mouse)-like 1 causes human retinal degeneration

Marion A. Maw<sup>+</sup>, Denis Corbeil<sup>1</sup>, Julia Koch<sup>1</sup>, Andrea Hellwig<sup>1</sup>, Jane C. Wilson-Wheeler, Robyn J. Bridges, Govindasamy Kumaramanickavel<sup>2</sup>, Sheila John<sup>2</sup>, Derek Nancarrow<sup>3</sup>, Katja Röper<sup>1</sup>, Anja Weigmann<sup>1</sup>, Wieland B. Huttner<sup>1</sup> and Michael J. Denton

Biochemistry Department, University of Otago, PO Box 56, Dunedin, New Zealand, <sup>1</sup>Department of Neurobiology, University of Heidelberg, Im Neuenheimer Feld 364, D-69120, Heidelberg, Germany and Max-Planck-Institute of Molecular Cell Biology and Genetics, Pfortenhauerstrasse 110, D-01307 Dresden, Germany, <sup>2</sup>Sankara Nethralaya, Medical Research Foundation, 18 College Road, Chennai, India and <sup>3</sup>Queensland Centre for Schizophrenia Research, Wolston Park Hospital, Brisbane, Australia

Received 23 August 1999; Revised and Accepted 15 October 1999

The disks of vertebrate photoreceptors are produced by outgrowths of the plasma membrane. Hence genes that encode retinal proteins targeted to plasma membrane protrusions represent candidates for inherited retinal degenerations. One such candidate is the gene encoding human prominin (mouse)-like 1 (PROML1, previously known as AC133 antigen) which belongs to the prominin family of 5-transmembrane domain proteins. Murine prominin (prom) shows a strong preference for plasma membrane protrusions in a variety of epithelial cells whereas PROML1 is expressed in retinoblastoma cell lines and adult retina. In the present study, molecular genetic analyses of a pedigree segregating for autosomal recessive retinal degeneration indicated that the affected individuals were homozygous for a nucleotide 1878 deletion in *PROML1*. This alteration is predicted to result in a frameshift at codon 614 with premature termination of translation. Expression of a similar prom deletion mutant in CHO cells indicated that the truncated protein does not reach the cell surface. Immunocytochemistry revealed that prom is concentrated in the plasma membrane evaginations at the base of the outer segments of rod photoreceptors. These findings suggest that loss of prominin causes retinal degeneration, possibly because of impaired generation of the evaginations and/or impaired conversion of the evaginations to disks.

## INTRODUCTION

Photoreceptors are the cells in the retina that are responsible for generating a neuronal signal in response to light. The outer segments of vertebrate photoreceptors house a stack of photoreceptive membranes called disks. These membranes have a high rate of turnover. In vertebrate rods, the disks are formed at the base of the outer segments initially by evagination of the plasma membrane with subsequent rim formation and membrane fusion resulting in release of individual disks into the cytoplasm. The disks are ultimately shed from the terminal end of the outer segment and phagocytosed by the retinal pigment epithelium. A similar, although not identical, process appears to occur in cone photoreceptive disks (1–3).

Inherited retinal degenerations represent a highly heterogeneous group of conditions. To date at least 114 loci and 51 genes with roles in a variety of cell biological processes have been implicated in these disorders (<http://www.sph.uth.tmc.edu/RetNet/>) (4). The

molecular biological events that occur during disk formation are poorly understood and so their potential roles in retinal degeneration remain largely unexplored. However, a disturbance in disk turnover might reasonably be expected to result in retinal degeneration. For example, it has been suggested that peripherin/rds, a protein located in the rims of disks and defective in cases of inherited retinal degeneration, may promote disk/plasma membrane fusion events (5,6).

The prominin 5-transmembrane domain glycoprotein is conserved throughout the animal kingdom, with representatives already identified in human, mouse, zebrafish, *Drosophila* and *Caenorhabditis elegans* (7–12). Prominin (prom) was originally identified as a protein that selectively localized at the apical surface of murine neuroepithelial cells (7) whereas PROML1 was identified as an antigenic marker (AC133 antigen) (8,13) in human hematopoietic stem cells and found to be expressed in retinoblastoma cell lines (13) and adult retina (7,8). Both prom (7,14) and PROML1 (D. Corbeil,

<sup>+</sup>To whom correspondence should be addressed. Tel: +64 3 479 5121; Fax: +64 3 479 7866; Email: marion.maw@stonebow.otago.ac.nz

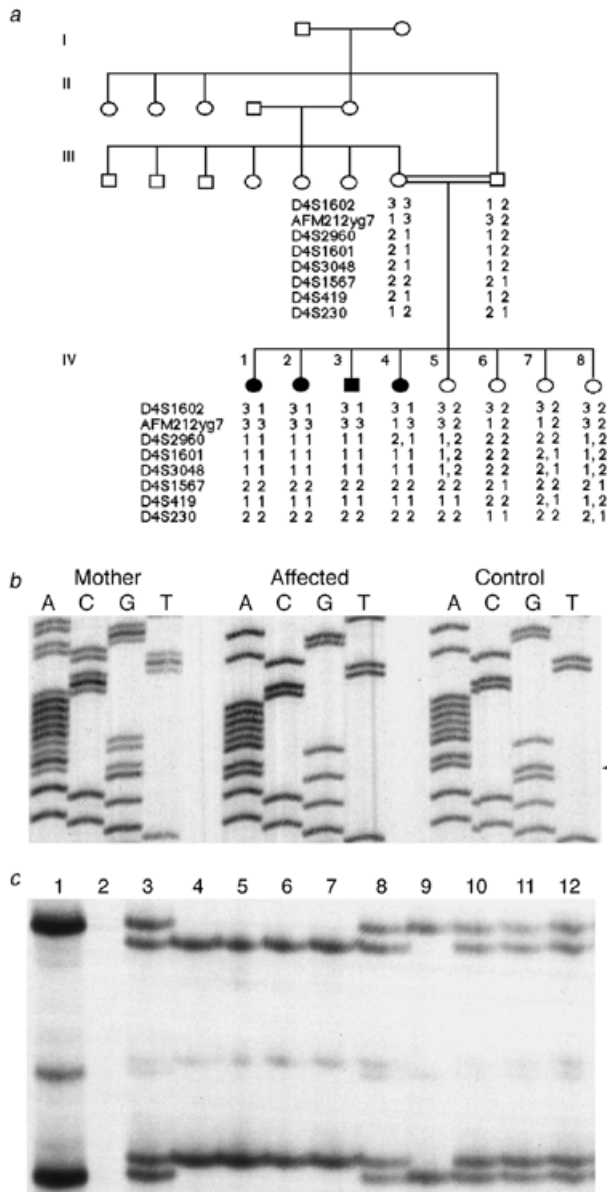


**Figure 1.** Molecular genetic analysis of Indian pedigree 166. (a) Segregation of autosomal recessive retinal degeneration and chromosome 4 markers. (b) Identification of a single base pair deletion at nucleotide 1878 (1878delG, arrow) of *PROML1*. Sequences are shown from the mother (heterozygous), affected individual IV-4 (homozygous) and an unrelated Indian control (homozygous normal). (c) Single-strand conformation polymorphism analysis of the exon containing nucleotide 1878, control (1), negative control (2), mother (3), affected siblings (4–7), unaffected siblings (8–11), father (12).

K. Röper, A. Hellwig, P. Simmons, D. Buck and W.B. Huttner, unpublished data) exhibit a profound preference for plasma membrane protrusions. These two proteins show an average of 60% amino acid sequence identity (9,10) and are likely to represent the murine and human orthologues.

Here we describe evidence that a frameshift mutation in the gene encoding *PROML1* is responsible for retinal degeneration in a consanguineous pedigree from India and that prom is concentrated in the plasma membrane evaginations at the base of the outer segments of murine rod photoreceptors.

## RESULTS

### Molecular genetic analysis of an Indian pedigree

Pedigree 166 contains an uncle–niece marriage that produced eight children, four of whom were affected by retinal degeneration (Fig. 1a). The affected individuals reported night blindness and loss of peripheral vision from childhood with progression to profound visual impairment and extinguished electroretinograms by their third decade. Fundus examination revealed narrowed arteries, optic disk pallor, pigment deposits and macular degeneration (Fig. 2a). One of these individuals (IV-2) also had polydactyly on one foot (Fig. 2b). Polydactyly and retinal degeneration are symptoms of Bardet Biedl syndrome (15); however, other features of that disorder were not evident in pedigree 166. The mother, at present in her sixth decade, reported poor vision in the left eye for the past 10 years and clinical examination revealed retinal degeneration in that eye (Fig. 2c and d). Because these symptoms were uniocular and had a late onset, we assumed that the mother was heterozygous for an autosomal recessive retinal degeneration allele.

Pedigree 166 is large enough to provide independent evidence of linkage and thereby locate the gene responsible for retinal degeneration in that family (16). Analysis of chromosome 4p markers (17,18) in DNA samples from pedigree 166 revealed that markers distal to D4S1602 formed a haplotype that co-segregated with autosomal recessive retinal degeneration (Fig. 1a). Crossovers in affected individual IV-4 and unaffected individual IV-5, respectively, indicated that the critical region was proximal to D4S2960 and distal to D4S1567. This region is distinct from the distal *PDEB* and proximal *CNCG* genes, both of which have previously been implicated in autosomal recessive retinal degeneration (19,20). Linkage with D4S3048 was excluded in an additional seven pedigrees from the Indian subcontinent segregating for non-syndromal autosomal recessive forms of retinal degeneration.

D4S1601 and D4S3048 map within intronic sequences of *PROML1* and the majority of that gene is contained in 23 exons distributed over >50 kb of genomic sequence from BAC clone COO24K08 (Table 1). *PROML1* is predicted to encode an 865 amino acid glycoprotein (8) and was considered to be a strong candidate gene for inherited retinal degeneration. PCR amplification of individual exons followed by DNA sequencing revealed a deletion of nucleotide 1878 in pedigree 166 (Fig. 1b). This alteration was associated with a single-strand conformation polymorphism that co-segregated with autosomal recessive retinal degeneration (Fig. 1c) and was not observed in 97 Indian control samples. Two-point analysis using this mutation as a rare polymorphism gave a peak lodscore of 3.17 at  $\theta = 0.00$ . The deletion is predicted to shift the reading frame from codon 614 onwards and result in premature termination of translation after addition of 12 amino acids unrelated to *PROML1* (Fig. 3a). The predicted protein would lack about half of the second extracellular loop, the final membrane spanning segment and the cytoplasmic C-terminal domain.

### Truncated prom does not reach the cell surface

A similar prom deletion mutant truncated at codon 623 (prom $\Delta$ ) (Fig. 3a) was expressed in CHO cells. In contrast to

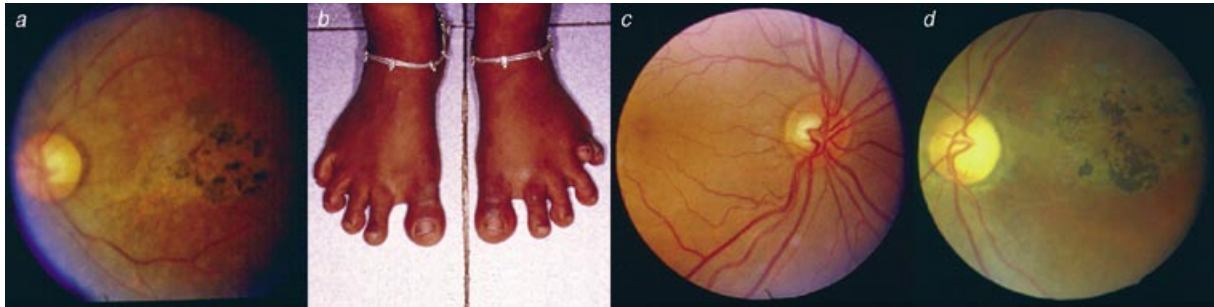


**Figure 2.** Clinical features in pedigree 166. (a) Affected individual IV-1, fundus. (b) Affected individual IV-2, polydactyly. (c) Mother, fundus of right eye. (d) Mother, fundus of left eye.

**Table 1.** Partial exon/intron structure of *PROML1*

Exon no.	Nucleotide no. in cDNA	3' splice site	5' splice site
1	547–667	tctgcagCATTGGCAT	CTCCAGAGgtaaaaac
2	668–731	ttttcagCAAATCAAA	TCTGAACAgtagtaa
3	732–821 D4S1601	gcatgtagGTATCAAT	GGCAACAGgtaagcag
4	822–1039	ttccatagCGATCAAG	TGAGGCAGgtgagcag
5	1040–1114	attttcagCTTCCACC	TCCAACAGgtatgctt
6	1115–1178	ttttcagGGCTATCA	CGTAGCAGgtgagatt
7	1179–1338	gtttcagGTATCAAA	TCATACTGgtgaggtt
8	1339–1491 D4S3048	ctctccagGTGGCTGG	CTCATGGTgtgaggtt
9	1492–1615	ttttccagTGGAGTTG	TATTCCGGgtaaatat
10	1616–1719	tgttctagGTTTTGGA	GTTTACAGgtatcaat
11	1720–1804	tcccacagTGA CTGCA	TTAATGAGgtaattag
12	1805–1948	tttcgacCATACTGG	TGGCTCAGgtatggcg
13	1949–2020	tattgtagACTGGTAA	ACAGTTTGgtgagttc
14	2021–2113	ttttgtagCCCCAGG	AATCACTGgtaacagt
15	2114–2167	cttgccagAGCACTCT	GATTGTTGgtaagggt
16	2168–2248	tctttcagGAGAGAGT	TTATTGAGgtgagcct
17	2249–2317	ctttccagGAAACTAA	AGTTCTCTgtaagtag
18	2318–2410	ccccctagATCAGTGA	ACCCCTTGgtaagatt
19	2411–2526	tttcctagAATTTGTT	TACGATGAgtaagtat
20	2527–2550	ttttatagTGTGAAA	ATGAAAAAgtaaagcct
21	2551–2619	tgttacagTATGGAAA	ATGACAAGgtaaaagca
22	2620–2659	ttttttagCCCATCAC	TGCTTGAGgtaagttt
23	2660–3794	catttcagCATCAGGA	poly(A)

The table summarizes BLAST analyses (27, <http://www.ncbi.nlm.nih.gov/BLAST/>) which produced matches for D4S1601, D4S3048 and the cDNA sequence for *PROML1* against genomic sequence from BAC clone COO24K08 (GenBank accession no. AC005598).

wild-type prom, prom $\Delta$  did not show any cell surface immunofluorescence on living cells with either monoclonal antibody (mAb) 13A4 or rabbit  $\alpha$ E3 antiserum (Fig. 3b). When fixed prom $\Delta$ -transfected cells were permeabilized with Triton X-100, a weak intracellular staining characteristic for the endoplasmic reticulum (ER) was detected with  $\alpha$ E3 antiserum, but not with mAb 13A4 (Fig. 3c) implying that the 13A4 epitope is deleted in prom $\Delta$ . No immunoreactive band corresponding to the deletion mutant was detected by immunoblotting with  $\alpha$ E3

antiserum (Fig. 3d). Recognition of the truncated protein by the sensitive immunofluorescence method in a typical ER pattern but not by immunoblotting suggests that prom $\Delta$  does not traffic out of the ER and therefore presumably is subject to ER degradation. Similar analyses were not performed with the human (rather than murine) mutant because AC133, the only available antibody to *PROML1*, recognizes a glycosylated structure (8) and hence is unlikely to be suitable for ER-to-cell surface transport studies.

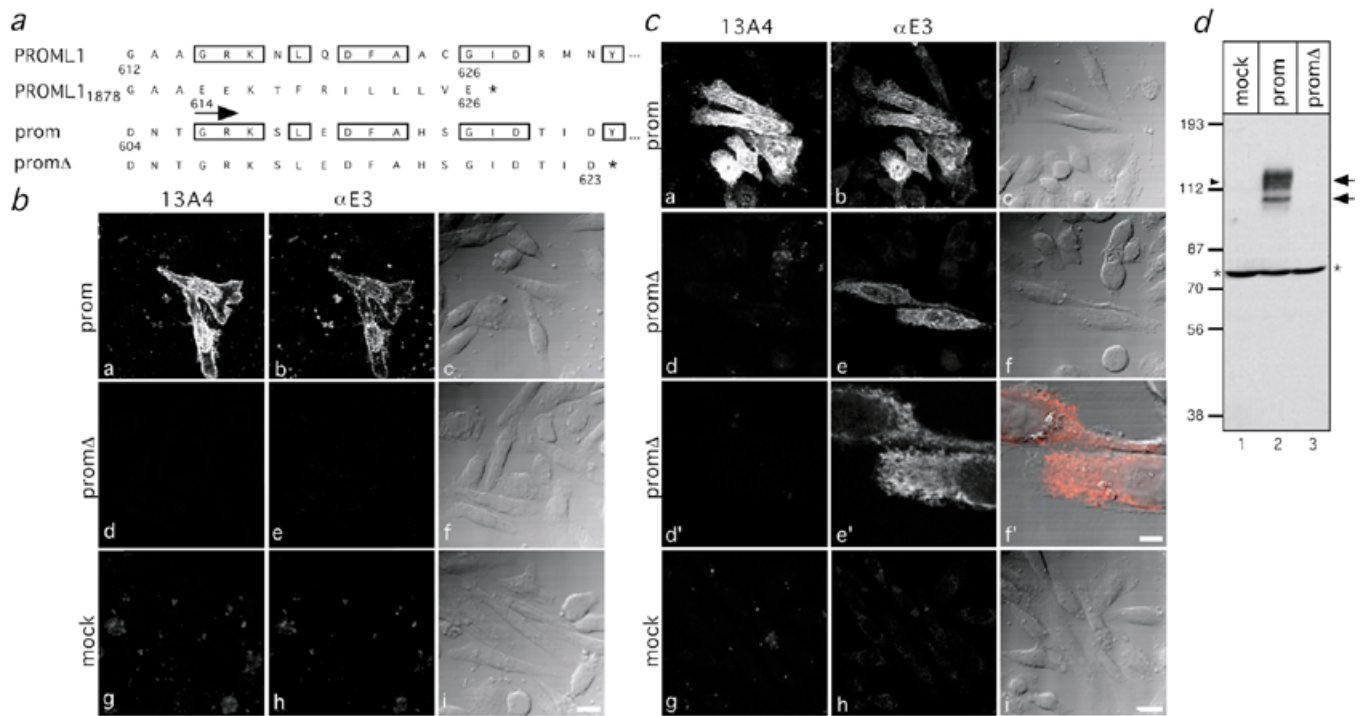


**Figure 3.** Truncated prominin does not reach the cell surface and is unstable. (a) Schematic representation of human prominin (mouse)-like 1 (PROML1) and mouse prominin (prom) and their C-terminal truncated forms, PROML1<sub>1878</sub> and prom $\Delta$ , respectively. Boxes show identical amino acid residues in corresponding sequence positions. The arrow indicates the frameshift position in PROML1<sub>1878</sub> followed by a premature stop codon. (b and c) Double immunofluorescence microscopy of prominin-transfected CHO cells. Intact (b) or paraformaldehyde-fixed, Triton X-100-permeabilized (c) CHO cells, transiently transfected with either wild-type prom [(b) a–c and (c) a–c], truncated mutant prom $\Delta$  [(b) d–f and (c) d–f and d'–f'] or vector DNA without insert (mock) [(b) g–i and (c) g–i], were incubated with the mAb 13A4 [13A4; (b) a, d and g and (c) a, d, d' and g] and the antiserum against the second extracellular loop [ $\alpha$ E3; (b) b, e and h and (c) b, e, e' and h], followed by appropriate fluorescein- and rhodamine-conjugated secondary antibodies and double immunofluorescence analysis using confocal microscopy. In all micrographs, except (c) d'–f', composite pictures of four optical sections are shown (bar, 10  $\mu$ m). In (c) d'–f', a high magnification view of a single optical section at the level of the coverslip is shown (bar, 3.5  $\mu$ m). (b) c, f and i and (c) c, f, f' and i: Nomarski; (c) f' is a merge of Nomarski and fluorescence of (c) e' (red). (d) Lysates from transfected CHO cells were analyzed by immunoblotting with  $\alpha$ E3 antiserum. The arrowhead points to the position of prominin present in mouse kidney (data not shown); arrows, prominin expressed in CHO cells; asterisks, non-specific immunoreactive band.

### Expression of prom in the murine retina

Immunoblot analysis of prom expression in the adult mouse eye using either mAb 13A4 (Fig. 4a) or  $\alpha$ E3 antiserum (data not shown) revealed immunoreactive bands of ~123 and 104 kDa, whereas a single band of 115 kDa was detected in adult mouse kidney. PNGase F-deglycosylation converted these bands to the same 94 kDa form, indicating that the difference between the 123, 104 and 115 kDa forms was due to differential N-glycosylation. The 123 and 115 kDa forms were resistant to endo H digestion whereas the 104 kDa form was again converted to the 94 kDa form (data not shown), suggesting that the 123 kDa form had passed through the Golgi apparatus and was present at the plasma membrane whereas the 104 kDa form was localized in the ER and the early Golgi. The ER/early Golgi-form of prom has been observed on ectopic expression in rapidly dividing cell lines (7,14); we speculate the presence of this form of prom may reflect high membrane turnover.

At the light microscopic level, prom immunoreactivity in the murine E10 (Fig. 4b–d) and E12 (data not shown) embryonic eye was observed in a layer where the surface of the progenitors to the photoreceptor cells meets the apical surface of the progenitors to the pigmented epithelial cells. In adult

murine retina, prom immunoreactivity was found in the layer containing the rod outer segments and microvilli of the pigmented epithelial cells, with the immunoreactivity being highest at the base of the rod outer segment (Fig. 4e and g). Immunogold electron microscopy showed that prom immunoreactivity was highest over the membrane evaginations of the rod outer segment, which are closest to the inner segment and represent the 'youngest' membranes in disk biogenesis, whereas the more distal region of the rod outer segment containing the disks was sparsely labeled (Fig. 5a–c). Gold particle density per unit area was  $17.4 \pm 7.7$  (SD,  $n = 19$ )-fold greater over evaginations than disks.

### DISCUSSION

Identification of the genes responsible for inherited retinal degeneration provides insights into both the cell biological processes of the healthy retina and the molecular pathological mechanisms that underlie the clinical symptoms. Our current findings suggest that a lack of functional PROML1 causes some cases of retinal degeneration in humans.

Linkage analysis with an intragenic marker excluded PROML1 as a cause of non-syndromal autosomal recessive retinal degeneration in an additional seven pedigrees from the

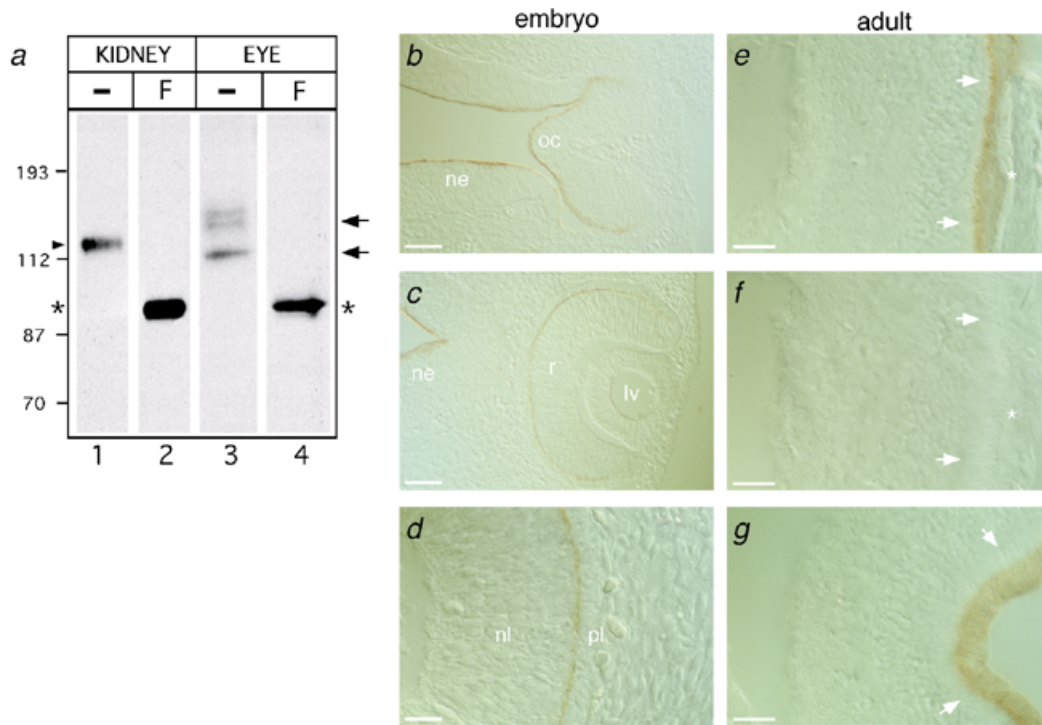


**Figure 4.** Expression and localization of prominin in the embryonic and adult mouse eye. (a) Lysates from adult mouse eyes (lanes 3 and 4, 100  $\mu$ g protein) and, for comparison, from adult kidney membranes (lanes 1 and 2, 25  $\mu$ g protein) were incubated in the absence (-) or presence of 1 U PNGase F (F) and analyzed by immunoblotting with mAb 13A4. Arrowhead, glycosylated 115 kDa form in kidney; arrows, glycosylated 123 and 104 kDa form in eye; asterisks, N-deglycosylated 94 kDa forms in kidney and eye. (b-g) Immunoperoxidase localization of prominin in the 10-day-old embryonic eye (b-d) and adult retina (e-g). Horizontal cryosections were incubated either with (b-e and g) or without (f) mAb 13A4 and observed using Nomarski optics. (b-d) ne, neuroepithelial cells; oc, optic cup; r, retina; lv, lens vesicle; nl, neural layer; pl, pigmented layer. (e-g) Arrows indicate the outer limiting membrane; asterisks show the pigmented cell layer. In (g), the layer of pigmented epithelial cells was lost during histological preparation. Bars in (b) and (c), 73  $\mu$ m; (d) 29  $\mu$ m; (e-g) 32  $\mu$ m.

Indian subcontinent. This finding suggests that mutations in *PROML1* are a rare cause of autosomal recessive retinal degeneration in that population. The locus for autosomal dominant Stargardt-like retinal degeneration in a Caribbean family was recently mapped within an  $\sim$ 12 cM critical region which encompasses *PROML1* (21); it remains to be determined whether a *PROML1* allele is responsible for that condition.

In the family reported here, the four siblings affected by an early-onset severe form of retinal degeneration were all homozygous for a *PROML1* frameshift allele. One of those siblings was also affected by polydactyly whereas the heterozygote mother manifested a unilateral, late-onset retinal degeneration with a similar fundal appearance. These additional symptoms may be coincidental but raise the possibility of variable penetrance and/or expressivity associated with the *PROML1* locus.

The process by which photoreceptive membranes are produced is poorly understood (1-3). The present study shows that prom is concentrated in the nascent photoreceptive membranes at the base of the outer segment of murine rod photoreceptors and that a prom deletion mutant mimicking the predicted human *PROML1* frameshift mutant does not reach the cell surface. Therefore, members of the prominin family may play a role in vertebrate photoreceptor disk morphogenesis. The absence of functional *PROML1* may impair: (i) the generation of plasma membrane evaginations in

the photoreceptor outer segment; and/or (ii) the membrane remodeling process occurring during subsequent formation of a disk rim and a closed disk. This impairment in turn may be the underlying cause of retinal degeneration in pedigree 166. Production of photoreceptive membranes in the invertebrate retina also involves generation of plasma membrane evaginations however disk formation does not occur (3). Perhaps comparison of the roles of prominin in the vertebrate and invertebrate retina may provide insights into the functional significance of these novel 5-transmembrane domain glycoproteins in plasma membrane protrusions.

## MATERIALS AND METHODS

### Molecular genetic analyses

Typing of microsatellite markers and single-strand conformation polymorphism analysis was done as previously described (22).

Intronic primer pairs for exons of *PROML1* (known as the gene encoding AC133 antigen) were designed from genomic sequence (GenBank accession no. AC005598) and used for PCR amplification of DNA samples from pedigree 166. PCR products were isolated using a High Pure PCR Product Purification kit (Boehringer Mannheim, Mannheim, Germany) and sequenced in both directions with a Thermo Sequenase radiolabeled terminator cycle sequencing kit (Amersham Life Science, Cleveland, OH). Primers used to amplify the exon

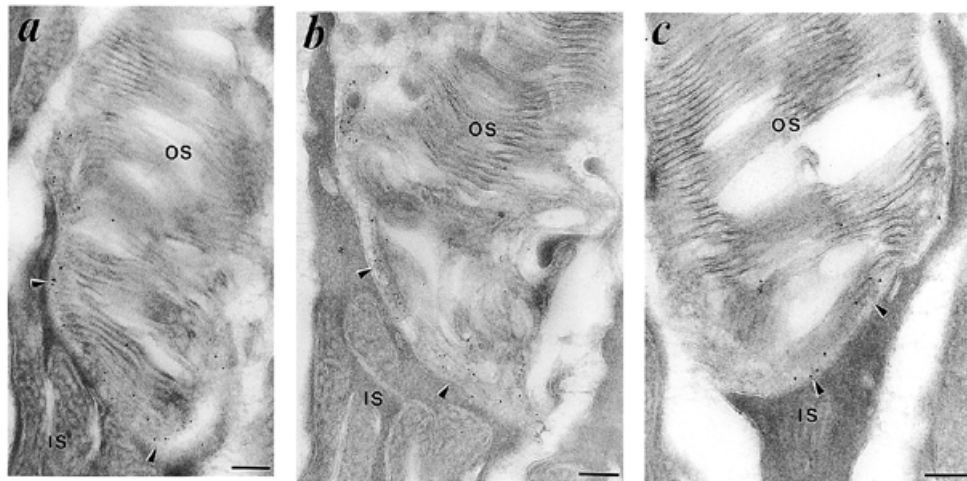


**Figure 5.** Immunogold electron microscopy showing the subcellular localization of prominin in murine rod photoreceptor cells. Ultrathin cryosections of the outer region of the retina containing the photoreceptor cell layer and pigment epithelium were stained with mAb 13A4 followed by rabbit anti-rat IgG/IgM and 9 nm protein A-gold. Three examples (a–c) showing prominin immunoreactivity predominantly at the base of the rod outer segment (arrowheads), sectioned approximately along its longitudinal axis, are depicted. OS, outer segment; IS, inner segment. Bar, 200 nm.

containing the mutation were 5'-CTAGGATTGCAG-GCATGAG-3' (forward) and 5'-TGAATGTACTCAAT-GCCACC-3' (reverse).

For single-strand conformation polymorphism analysis, the primers used to generate a PCR product containing the mutation were 5'-GCATACTGGAAGCATAAGCAG-3' (forward) and 5'-GATCAAGCATGAACACATGCG-3' (reverse). The single-strand conformation polymorphism gelshift that segregated with arRD within pedigree 166 was not present in 97 Indian controls (194 chromosomes). Two-point linkage analysis was done with MLINK version 5.10 (23), assuming a gelshift allele frequency of 0.01 and fully penetrant arRD with a disease frequency of 0.015 (24).

#### Plasmid construction and transfection

The bacterial expression plasmid pGEX-E3, containing the mouse prom cDNA from nt 1686 to 2543 fused in-frame to glutathione *S*-transferase (GST), was constructed by selective PCR amplification of a composite cDNA [derived from clones 3Ab1 and 4B (7)]. The oligonucleotides 5'-CTTACGTTT-GGATCCGGTGCAAATG-3' and 5'-CCTATGCGGATCCGA-ACTAATTTCAG-3' were used as 5' and 3' primers, respectively. Both oligonucleotides created a *Bam*HI restriction site and the 3' primer in addition introduced a TAG stop codon. The resulting PCR fragment was digested with *Bam*HI and cloned into the corresponding site of pGEX-2t (Pharmacia, Freiburg, Germany). The GST-fusion protein, derived from the pGEX-E3 plasmid, was purified and used to generate a rabbit antiserum against the E3 fragment of prominin (residues Gly500–Asn785, corresponding to the second extracellular loop), as described previously (14).

The eukaryotic expression plasmid pRc/CMV-prominin, containing a mouse prom cDNA (entire open reading frame), has been described previously (7). The C-terminally truncated form of mouse prom was obtained by ligating a double-stranded oligonucleotide into the pRc/CMV-prominin plasmid opened with *Cla*I and *Apa*I. The double-stranded oligonucleo-

tide, which introduced a translational stop codon (TGA) at the amino acid position 624, was created by annealing the phosphorylated oligonucleotides 5'-CGATTGAAAGCTTCTAG-GGCC-3' (forward) and 5'-CTAGAAGCTTTCAAT-3' (reverse). All constructs were confirmed by sequencing.

CHO cells were cultured as described previously (14) and transiently transfected with the prominin eukaryotic expression plasmids using the lipofectaMINE reagent (Gibco BRL, Gaithersburg, MD) according to the supplier's instructions. After 48 h the medium was changed, sodium butyrate was added to a final concentration of 10 mM, and the cells were incubated for another 17 h. Transfected cells were then used for immunofluorescence, or were solubilized in ice-cold solubilization buffer 1 (2% Triton X-100, 0.1% SDS, 150 mM NaCl, 5 mM EGTA, 50 mM Tris–HCl pH 7.5, 1 mM PMSF, 2 µg/ml leupeptin, 10 µg/ml aprotinin), and extracts obtained after centrifugation (10 min, 10 000 g, 4°C) were subjected to SDS–PAGE and immunoblotting.

#### Endoglycosidase digestion and immunoblotting

Whole eyes were dissected from adult mouse (NMRI strain), rinsed several times in ice-cold PBS containing 10 mM PMSF, and then homogenized in 500 µl of solubilization buffer 2 (1% Triton X-100, 0.1% SDS, 25 mM EDTA, 1% 2-mercaptoethanol, 50 mM sodium phosphate pH 7.2, 1 mM PMSF, 2 µg/ml leupeptin, 10 µg/ml aprotinin) at 4°C with an Eppendorf plastic homogenizer. Homogenates were kept on ice for 30 min and insoluble material was then removed in a microcentrifuge (10 min, 10 000 g). An aliquot of the extract corresponding to one-eighth of one eye was incubated overnight at 37°C in the absence or presence of 1 U PNGase F according to the manufacturer's protocol (Boehringer Mannheim). Proteins were analyzed by SDS–PAGE and immunoblotting as described previously (14) using either mAb 13A4 (7) (1 µg/ml) or αE3 antiserum (1:5000) as primary antibodies.

## Immunofluorescence and confocal microscopy

Indirect immunofluorescence microscopy analysis of intact and permeabilized cells were performed essentially as described (14), except that Triton X-100 (0.3%, 10 min) was used as the permeabilizing agent. The cells were double labeled with mAb 13A4 (10 µg/ml) and αE3 antiserum (1:300) followed by dichlorotriazinyl amino fluorescein-conjugated anti-mouse secondary antibody and Lissamine Rhodamine-conjugated anti-rabbit secondary antibody (Jackson ImmunoResearch Laboratories, West Grove, CA). The cells were observed with a Leica TCS<sup>4D</sup> confocal laser scanning microscope.

## Light and electron microscopy

**Light microscopy.** Ten-day-old mouse embryos (NMRI strain) were fixed by immersion in 4% paraformaldehyde and 4% sucrose in PBS overnight at 4°C. Adult eyes were dissected from male mice perfused with 4% paraformaldehyde, and were postfixed as above. After infiltration with 30% sucrose in PBS the tissues were embedded in Tissue-Tek (Miles, Kankakee, USA) and frozen. Cryosections (10 µm) were mounted on 3-aminopropyltriethoxysilane (Sigma, St Louis, MO)-coated glass slides. Triton X-100-permeabilized sections were treated with 0.5% H<sub>2</sub>O<sub>2</sub> in methanol to inhibit endogenous peroxidases and blocked with 1% fatty acid free bovine serum albumin (BSA; Sigma), 0.1% Triton X-100 in PBS. Incubation with mAb 13A4 (12 µg/ml) was performed overnight at 4°C followed by incubation with biotin-SP-conjugated donkey anti-rat IgG (Jackson ImmunoResearch Laboratories) for 1 h at room temperature. The ABC reagent (Vectastain) was used to reveal the antigen-antibody complexes according to manufacturer's instructions and the color reaction was performed with diaminobenzidine (Sigma). Stained sections were observed with a Zeiss Axiophot using Nomarski optics.

**Immunoelectron microscopy.** Eyes of adult mice were fixed with 8% paraformaldehyde in 0.2 M HEPES-NaOH buffer pH 7.4 overnight at 4°C. Tissue pieces (eyecups) were then infiltrated with 15% polyvinylpyrrolidone, 1.95 M sucrose in PBS (25), and ultrathin cryosections (26) were cut at -100°C with a Reichert FCS cryo-ultramicrotome (Leica, Vienna, Austria). Cryosections were picked up using 2.3 M sucrose and mounted on Formvar/carbon-coated grids. Sections were quenched with 20 mM glycine in PBS for 10 min, blocked with 0.5% BSA/0.1% gelatin in PBS for 10 min, and sequentially incubated with the mAb 13A4 (250 µg/ml), rabbit anti-rat antibody (Jackson ImmunoResearch Laboratories) and protein A-gold (9 nm), each in blocking solution. After several washing steps with the blocking solution and PBS, sections were postfixed with 1% glutaraldehyde in PBS for 10 min at room temperature, washed extensively in distilled water, treated with 0.3% uranyl acetate/1.8% methyl cellulose, and air-dried. The immunogold-labeled sections were examined by electron microscopy (EM 10; Zeiss, Oberkochen, Germany).

**Quantification of gold particle density.** Using prints of electron micrographs of immunogold-labeled cryosections, gold particles were counted, for each of 19 individual rod outer segments, over the membrane evaginations and the membrane

disks present on the entire print. The areas containing the membrane evaginations and membrane disks analyzed were determined by weighing the corresponding paper of the print. Larger holes between membrane profiles, generated by the preparation of cryosections, were excluded. For each rod outer segment (i.e. print), the number of gold particles per unit area over evaginations and disks was calculated and the ratio evaginations:disks determined.

## ACKNOWLEDGEMENTS

We thank the families participating in the study. M.A.M., J.C.W.-W., R.J.B. and M.J.D. were supported by the New Zealand Health Research Council, United States Foundation Fighting Blindness, New Zealand Lottery Grants Board, Australian Retinitis Pigmentosa Association, Retina NZ Inc. and the Royal NZ Foundation Fighting Blindness. D.C. was the recipient of a postdoctoral fellowship from the Max-Planck-Society, J.K. and A.W. were recipients of predoctoral fellowships from the Deutsche Forschungsgemeinschaft (Graduiertenkolleg Molecular and Cellular Neurobiology), K.R. was supported by the Studienstiftung des Deutschen Volkes, and W.B.H. was the recipient of grants from the Deutsche Forschungsgemeinschaft (SFB 317, SFB 352).

## REFERENCES

- Steinberg, R.H., Fisher, S.K. and Anderson, D.H. (1980) Disc morphogenesis in vertebrate photoreceptors. *J. Comp. Neurol.*, **190**, 501–518.
- Corless, J.M. and Fetter, R.D. (1987) Structural features of the terminal loop region of frog retinal rod outer segment disk membranes: III. Implications of the terminal loop complex for disk morphogenesis, membrane fusion, and cell surface interactions. *J. Comp. Neurol.*, **257**, 24–38.
- Williams, D.S. (1991) Actin filaments and photoreceptor membrane turnover. *Bioessays*, **13**, 171–178.
- Inglehearn, C.F. (1998) Molecular genetics of human retinal dystrophies. *Eye*, **12**, 571–579.
- Arikawa, K., Molday, L.L., Molday, R.S. and Williams, D.S. (1992) Localization of peripherin/*rds* in the disk membranes of cone and rod photoreceptors: relationship to disk membrane morphogenesis and retinal degeneration. *J. Cell Biol.*, **116**, 659–667.
- Boesze-Battaglia, K., Lamba, O.M., Napoli, A.A., Sinha, S. and Guo, Y. (1998) Fusion between retinal rod outer segment membranes and model membranes: a role for photoreceptor peripherin/*rds*. *Biochemistry*, **37**, 9477–9487.
- Weigmann, A., Corbeil, D., Hellwig, A. and Huttner, W. (1997) Prominin, a novel microvilli-specific polytopic membrane protein of the apical surface of epithelial cells, is targeted to plasmalemmal protrusions of non-epithelial cells. *Proc. Natl Acad. Sci. USA*, **94**, 12425–12430.
- Miraglia, S., Godfrey, W., Yin, A.H., Atkins, K., Warnke, R., Holden, J.T., Bray, R.A., Waller, E.K. and Buck, D.W. (1997) A novel five-transmembrane hematopoietic stem cell antigen: isolation, characterization, and molecular cloning. *Blood*, **90**, 5013–5021.
- Corbeil, D., Röper, K., Weigmann, A. and Huttner, W.B. (1998) AC133 hematopoietic stem cell antigen: human homologue of mouse kidney prominin or distinct member of a novel protein family? *Blood*, **91**, 2625–2626.
- Miraglia, S., Godfrey, W. and Buck, D. (1998) A response to AC133 hematopoietic stem cell antigen: human homologue of mouse kidney prominin or distinct member of a novel protein family? *Blood*, **91**, 4390–4391.
- Corbeil, D., Röper, K. and Huttner, W.B. (1999) Identification and sequence analysis of a *Drosophila* ortholog of mouse prominin and human AC133 antigen. In press (GenBank accession no. AF127935).

12. Corbeil, D., Treichel, J., Röper, K., Brand, M. and Huttner, W.B. (1999) Sequence analysis of a zebrafish ortholog of mouse prominin and human AC133 antigen. In press (GenBank accession no. AF160970).
13. Yin, A.H., Miraglia, S., Zanjani, E.D., Almeida-Porada, G., Ogawa, M., Leary, A.G., Olweus, J., Kearney, J. and Buck, D.W. (1997) AC133, a novel marker for human hematopoietic stem and progenitor cells. *Blood*, **90**, 5002–5012.
14. Corbeil, D., Röper, K., Hannah, M.J., Hellwig, A. and Huttner, W.B. (1999) Selective localization of the polytopic membrane protein prominin in microvilli of epithelial cells—a combination of apical sorting and retention in plasma membrane protrusions. *J. Cell Sci.*, **112**, 1023–1033.
15. Riise, R., Andreasson, S., Wright, A.F. and Tornqvist, K. (1996) Ocular findings in the Laurence-Moon-Bardet-Biedl syndrome. *Acta Ophthalmol.*, **74**, 612–617.
16. Chand, A., Kumaramanickavel, G., Abraham, M., Gahlot, D.K., Apte, B.N. and Denton, M.J. (1991) Indian pedigrees with recessive retinitis pigmentosa: potential for homozygosity mapping. In Humphries, P., Bhattacharya, S. and Bird, A. (eds), *Degenerative Retinopathies: Advances in Clinical and Genetic Research*. CRC Press, Boca Raton, FL, pp. 35–40.
17. Dib, C., Faure, S., Fizames, C., Samson D., Drouot, N., Vignal, A., Millasseau, P., Marc, S., Hazan, J., Seboun, E., Lathrop, M., Gyapay, G., Morissette, J. and Weissenbach, J. (1996) A comprehensive map of the human genome based on 5,264 microsatellites. *Nature*, **380**, 152–154.
18. Information for AFM212yg7. Human Physical Mapping Project, The Whitehead Institute for Biomedical Research/MIT Center for Genome Research (<http://www-genome.wi.mit.edu/>).
19. McLaughlin, M.E., Sandberg, M.A., Berson, E.L. and Dryja, T.P. (1993) Recessive mutations in the gene encoding the  $\beta$ -subunit of rod phosphodiesterase in patients with retinitis pigmentosa. *Nature Genet.*, **4**, 130–134.
20. Dryja, T.P., Finn, J.T., Peng, Y.W., McGee, T.L., Berson, E.L. and Yau, K.W. (1995) Mutations in the gene encoding the alpha subunit of the rod cGMP-gated channel in autosomal recessive retinitis pigmentosa. *Proc. Natl Acad. Sci. USA*, **92**, 10177–10181.
21. Kniazeva, M., Chiang, M.F., Morgan, B., Anduze, A.L., Zack, D.J., Han, M. and Zhang, K. (1999) A new locus for autosomal dominant Stargardt-like disease maps to chromosome 4. *Am. J. Hum. Genet.*, **64**, 1394–1399.
22. Maw, M., Kumaramanickavel, G., Kar, K., John, S., Bridges, R. and Denton, M.J. (1998) Two Indian siblings with Oguchi disease are homozygous for an arrestin mutation encoding premature termination. *Hum. Mutat.*, **1**(suppl.), S317–S319.
23. Lathrop, G.M., Lalouel, J.M., Julier, C. and Williams, D.S. (1985) Multilocus linkage analysis in humans: detection of linkage and estimation of recombination. *Am. J. Hum. Genet.*, **37**, 482–498.
24. Knowles, J.A., Shugart, Y., Banerjee, P., Gilliam, T.C., Lewis, C.A., Jacobson, S.G. and Ott, J. (1994) Identification of a locus, distinct from RDS-peripherin, for autosomal recessive retinitis pigmentosa on chromosome 6p. *Hum. Mol. Genet.*, **3**, 1401–1403.
25. Tokuyasu, K.T. (1989) Use of poly(vinylpyrrolidone) and poly(vinyl alcohol) for cryoultramicrotomy. *Histochem. J.*, **21**, 163–171.
26. Griffiths, G. (1993) *Fine Structure Immunocytochemistry*. Springer, Heidelberg, Germany.
27. Altschul, S.F., Gish, W., Miller, W., Myers, E.W. and Lipman, D.J. (1990) Basic local alignment search tool. *J. Mol. Biol.*, **215**, 403–410.